



Open Access

ORIGINAL ARTICLE

Male Health

Effect of thermophilic bacterium HB27 manganese superoxide dismutase in a rat model of chronic prostatitis/chronic pelvic pain syndrome (CP/CPPS)

Nai-Wen Chen^{1,2,*}, Jing Jin^{2,*}, Hong Xu^{1,2}, Xue-Cheng Wei^{1,2}, Ling-Feng Wu², Wen-Hua Xie², Yu-Xiang Cheng^{2,3}, Yi He², Jin-Lai Gao⁴

We investigated the therapeutic effects of superoxide dismutase (SOD) from thermophilic bacterium HB27 on chronic prostatitis/chronic pelvic pain syndrome (CP/CPPS) and its underlying mechanisms. A Sprague–Dawley rat model of CP/CPPS was prepared and then administered saline or *Thermus thermophilus* (Tt)-SOD intragastrically for 4 weeks. Prostate inflammation and fibrosis were analyzed by hematoxylin and eosin staining, and Masson staining. Alanine transaminase (ALT), aspartate transaminase (AST), serum creatinine (CR), and blood urea nitrogen (BUN) levels were assayed for all animals. Enzyme-linked immunosorbent assays (ELISA) were performed to analyze serum cytokine concentrations and tissue levels of malondialdehyde, nitric oxide, SOD, catalase, and glutathione peroxidase. Reactive oxygen species levels were detected using dichlorofluorescein diacetate. The messenger ribonucleic acid (mRNA) expression of tissue cytokines was analyzed by reverse transcription polymerase chain reaction (RT-PCR), and infiltrating inflammatory cells were examined using immunohistochemistry. Nuclear factor- κ B (NF- κ B) P65, P38, and inhibitor of nuclear factor- κ B α (I- κ B α) protein levels were determined using western blot. Tt-SOD significantly improved histopathological changes in CP/CPPS, reduced inflammatory cell infiltration and fibrosis, increased pain threshold, and reduced the prostate index. Tt-SOD treatment showed no significant effect on ALT, AST, CR, or BUN levels. Furthermore, Tt-SOD reduced inflammatory cytokine expression in prostate tissue and increased antioxidant capacity. This anti-inflammatory activity correlated with decreases in the abundance of cluster of differentiation 3 (CD3), cluster of differentiation 45 (CD45), and macrophage inflammatory protein 1 α (MIP1 α) cells. Tt-SOD alleviated inflammation and oxidative stress by reducing NF- κ B P65 and P38 protein levels and increasing I- κ B α protein levels. These findings support Tt-SOD as a potential drug for CP/CPPS.

Asian Journal of Andrology (2021) 23, 323–331; doi: 10.4103/aja202157; published online: 02 November 2021

Keywords: chronic pelvic pain syndrome; chronic prostatitis; superoxide; thermophilic bacterium

INTRODUCTION

Prostatitis is a common urological clinical disease. According to the National Institutes of Health 1995 prostatitis classification method, prostatitis can be divided into four types: type I, acute bacterial prostatitis; type II, chronic bacterial prostatitis; type III, chronic prostatitis/chronic pelvic pain syndrome (CP/CPPS); and type IV, asymptomatic prostatitis. Type III can be subclassified as inflammatory (type IIIa) and non-inflammatory (type IIIb) subtypes. Patients with the IIIa subtype have an increased number of leukocytes in expressed prostatic secretion (EPS), semen, and post-prostatic massage urine (VB3). In contrast, the leukocyte count in EPS, semen, and VB3 of patients with the IIIb subtype are within the normal range.¹ CP/CPPS has the highest incidence among the four types, accounting for approximately 90%–95% of patients with prostatitis, and is the most common urological disease in men under 50 years of age.² The main symptoms of CP/CPPS include long-term perineal and lower

abdominal pain, abnormal urination, and neuropsychiatric symptoms such as sexual dysfunction and reduced fertility.^{3,4} Clinically, CP/CPPS is characterized by slow onset, stubborn symptoms, recurrent attacks, and lingering difficulty in healing, which seriously affects the quality of life of patients.⁵ Currently, the treatment of CP/CPPS mainly involves symptom relief but does not completely cure the disease.⁶ Importantly, the pathogenesis and pathophysiological changes occurring in CP/CPPS are unclear, and may be related to oxidative stress, pathogenic bacterial infection, and neurological, immune, and endocrine system dysfunction.^{6–8}

Recent studies have also shown that CP/CPPS is considered an autoimmune disease, with oxidative stress and inflammation playing important roles in its pathogenesis.⁹ Oxidative stress is a state in which oxidation and antioxidant effects are imbalanced, favoring oxidation in the body, which can lead to tissue infiltration of inflammatory neutrophils that promote the production of reactive oxygen species

¹Department of Surgery, The Second Clinical Medical College of Zhejiang Chinese Medical University, Hangzhou 310000, China; ²Department of Urology, The Affiliated Hospital of Jiaxing University, Jiaxing 314000, China; ³Department of Surgery, Bengbu Medical College, Bengbu 233000, China; ⁴Department of Pharmacology, College of Medical, Jiaxing University, Jiaxing 314000, China.

*These authors contributed equally to this work.

Correspondence: Dr. Y He (heyi@zjxu.edu.cn) or Dr. JL Gao (gaojinlai@zjxu.edu.cn)

Received: 05 April 2021; Accepted: 17 August 2021

(ROS) and reactive nitrogen species-free radicals.^{10,11} Thus, antioxidants or anti-inflammatory drugs may be useful as therapeutic agents for treating CP/CPPS. As an antioxidant, superoxide dismutase (SOD) can catalyze and remove excess cellular ROS, which protects cells from oxidative damage caused by free radicals, maintain the balance of oxygen free radicals, and reduce inflammation.^{12,13} Although many studies have shown that SOD removes excess ROS from tissues, the therapeutic effects of ordinary SODs remain unsatisfactory, possibly because of their instability in high temperature, acidic, or alkaline environments, or following exposure to digestive enzymes.^{14,15}

Thermus thermophilic (Tt)-SOD from thermophilic *Thermus* HB27 shows excellent stability and activity under high temperature, high pH, digestion with pepsin, trypsin, and other proteases, and has great development value.¹⁶ Therefore, the aim of this study was to investigate whether Tt-SOD could remove excess ROS and reduce inflammatory cell infiltration in a rat model of CP/CPPS to alleviate the symptoms of CP/CPPS and to explore the potential mechanisms of Tt-SOD activity.

MATERIALS AND METHODS

Reagents

The following reagents were purchased from the indicated companies: Tt-SOD (Hangzhou Redox Pharmatech, Hangzhou, China); complete Freund's adjuvant (CFA; Sigma, St. Louis, MO, USA); SOD, catalase (CAT), glutathione peroxidase (GSH-PX), and malondialdehyde (MDA; Nanjing Jiancheng Institute of Biotechnology, Nanjing, China); nitric oxide (NO) assay kit (Beyotime Biotechnology, Shanghai, China); 2,7'-dichlorofluorescein diacetate (DCFH-DA) ROS Assay Kit (Baiao Lai Bo Technology Co., Ltd., Beijing, China); interleukin (IL)-1 β and tumor necrosis factor (TNF)- α enzyme-linked immunosorbent assays (ELISA) kits (R&D Systems, Minneapolis, MN, USA); IL-8 ELISA kit (Westang, Shanghai, China); Masson trichrome staining kit (KeyGen Biotech, Nanjing, China); anti-cluster of differentiation 3 (CD3), anti-CD45, and anti-glyceraldehyde-3-phosphate dehydrogenase (GAPDH) antibodies (Abcam, Cambridge, UK); anti-macrophage inflammatory protein 1 α (MIP1 α) antibody (Mybiosource, San Diego, CA, USA); anti-nuclear factor (NF)- κ B p65, anti-phospho-NF- κ B p65, anti-p38-mitogen-activated protein kinase (MAPK), anti-phospho-p38-MAPK antibodies, and anti-inhibitor of nuclear factor- κ B α (I- κ B α) antibody (Cell Signaling Technology, Danvers, MA, USA); and Total RNA Kit (Tiangen Biotech, Beijing, China) and a reverse transcription polymerase chain reaction (RT-PCR) kit (Bio-Rad, Hercules, CA, USA).

Forty male Sprague–Dawley rats were purchased from Shanghai Regen Biotechnology (Shanghai, China), and then rested for a week. Rats were housed at 25°C \pm 3°C, exposed to an alternating 12-h light and 12-h dark cycle, and provided free access to food and water.

Experimental design

The 40 Sprague–Dawley rats were randomly divided into five groups with eight rats in each: blank sham (control), model, Tt-SOD low-dose (100 U g⁻¹), medium-dose (300 U g⁻¹), and high-dose (500 U g⁻¹) groups. We induced CP/CPPS as described by Peng *et al.*,¹⁷ which is one of the most commonly used methods for producing models of CP/CPPS induction. Briefly, the rats were first intraperitoneally anesthetized with 10% chloral hydrate (1 ml per 300 g), and then abdominal hair was shaved, skin disinfected, and lower abdomen cut at the midline to expose the prostate. Rats in the model and Tt-SOD additive groups were injected with 0.1 ml CFA into the prostate, and the abdominal incision was sutured layer by layer. In the sham group,

only the prostate was turned several times after laparotomy and then the abdomen was closed. On the 2nd day after successful modeling, the model and Tt-SOD groups were administered 1 ml of normal saline or Tt-SOD orally for 4 consecutive weeks, whereas the sham group did not receive any treatment. On day 28, blood samples were collected from the abdominal aorta under 10% chloral hydrate anesthesia. After centrifugation (Xiangyi, Hunan, China) at 2000g for 15 min, the supernatant was collected and stored at -80°C for subsequent biochemical tests. Simultaneously, prostates were quickly removed and cleaned with normal saline to remove adipose tissue and adhered blood. The wet weights of prostates were recorded, a part of the prostates was used for histological imaging, and a part was stored at -80°C for biochemical analysis. Finally, at the end of the experiment, the rats were euthanized by inhalation of excessive amounts of isoflurane. The study was carried out as per the Regulations for the Administration of Affairs Concerning Experimental Animals and consented by the Experimental Animal Ethics Committee of the Affiliated Hospital of Jiaxing University (Jiaxing, China; ethics approval number: JUMC2021-077).

Prostatic index determination

On day 28 after surgery, the weight of rats in each group was recorded after anesthesia with 10% chloral hydrate, the total weight of the abdominal and dorsolateral portions of the prostate was measured, and the prostate index (PI) was calculated as follows: PI = (prostate weight [in g]/rat weight [in g]) \times 10 000.¹⁸

Pain threshold assessment

Pain threshold tests were performed on rats 1 day before surgery and 7 days, 14 days, and 28 days after surgery as described by Cheng *et al.*¹⁹ and Ni *et al.*²⁰ The scrotum of rats was stimulated vertically by Von Frey filaments (BME-404, Institute of Biological Medicine, Academy of Medical Science, Beijing, China) continuously five times for at least 10 s each time. Sharp abdominal contractions, scratching, jumping, and licking of the stimulated area were considered as pain thresholds, and the average value was recorded.

Evaluation of serum pro-inflammatory mediators

Serum samples were collected, and the levels of TNF- α , IL-1 β , and IL-8 were determined by ELISA according to the manufacturer's instructions and previous studies.²¹

Evaluation of serum biochemical parameters

From each rat, 500 μ l of serum was collected for the analysis of biochemical parameters. Serum creatinine (CR), blood urea nitrogen (BUN), alanine transaminase (ALT), and aspartate transaminase (AST) levels were measured using an automatic biochemical analyzer (Olympus, Tokyo, Japan).

Hematoxylin and eosin (H&E) staining

Prostate tissue was first fixed in 4% paraformaldehyde for 24 h and then embedded in paraffin wax. Sections (5 μ m thick) were stained with H&E for morphological examination of the prostate tissue. Briefly, the sections were dewaxed, stained, dehydrated, and sealed according to the instructions of the H&E staining kit (Beyotime Biotechnology). Images were observed under a light microscope (400 \times magnification; CKX53, Olympus), and a representative field of view was selected for imaging.

Masson staining

Prostate tissue was processed as described above. After fixation, paraffin-embedding, and sectioning of the prostate tissue, a Masson's trichrome staining kit (KeyGen Biotech, Nanjing, China) was used, and fibrosis of the prostate tissue was observed. Briefly, following

instructions, the slices were dewaxed, dyed, rinsed, dehydrated, dried, and separately sealed. Images were observed under a light microscope (400× magnification), and a representative field of view was selected for imaging.

Immunohistochemical (IHC) examination

IHC staining was performed following the manufacturer's instructions. Briefly, paraffin-embedded slices from each group were dried in an oven for 3 h. After drying and conventional xylene dewaxing, the slides were subjected to graded alcoholization followed by hydration. Citric acid antigenic repair solution was applied, and then the slides were incubated with 3% H₂O₂ at room temperature for 10 min to inactivate endogenous enzymes. Normal goat serum was used for blocking for 10 min. Diluted antibodies (CD3 antibody [1:50], CD45 antibody [1:200], and MIP1α antibody [1:100]) were added to the slides for overnight incubation at 4°C. Next, the polymer enhancer and horseradish peroxidase-labeled anti-pika polymer were added for 20 min and 10 min, respectively. Finally, 3,3'-diaminobenzidine was used for color development; the reaction time was controlled by observation under a microscope, and the sections were stained with hematoxylin solution. After drying, the sections were sealed with gum. IHC readings were blindly performed by two experienced researchers. Each IHC section was observed and photographed under a microscope (Leica TCS SP8, Leica, Solms, Germany) at a magnification of 400×, and semi-quantitative analysis was performed using integral optical density analysis.

ROS fluorescent probe

ROS generation was measured using DCFH-DA as previously described.²² Briefly, prostate samples from each group were placed in 4% paraformaldehyde fixation solution for 24 h and then transferred to 30% sucrose for dehydration for 48 h. Tissue blocks were then placed in a small box and optimal cutting temperature compound (OCT)-embedding agent was added to immerse the tissues; the box was slowly placed into a small cup containing liquid nitrogen. Once the bottom of the box was in contact with the liquid nitrogen, it was left in place and not further immersed. The tissue froze rapidly (approximately 10 s). After preparing the frozen blocks, the samples were sliced in a freezer slicer. Next, cleaning working liquid was spread over the surface of the slices at room temperature and carefully removed after 10 min. Finally, DCFH-DA staining solution (50 μmol l⁻¹) was added to the frozen sections, incubation was continued at 37°C for 20 min, and fluorescence microscope (Leica) observation and photography were performed (630× magnification; green, DCFH-DA; blue, 4',6'-diamidino-2-phenylindole [DAPI]).

Homogenate preparation

Prostate samples were weighed and divided into two parts before adding sterile normal saline (for ELISA) or radioimmunoprecipitation (RIPA) lysate (for western blot). Tissue homogenates were prepared using a tissue homogenizer at 4°C, centrifuged at 10 000g for 10 min (3K15, Sigma, Osterode am Harz, Germany), and the supernatant was collected and stored at -20°C.

Assessment of oxidative stress levels

An appropriate amount of sample homogenate was used to quantify SOD, MDA, GSH-PX, NO, and CAT levels following the instructions of the ELISA kit. Specific steps were performed as described previously.^{23,24}

RT-PCR analysis

Total RNA was extracted and reverse-transcribed using kits as previously described; quantitative PCR was performed using a

LightCycler 480 Real-time PCR System (LightCycler 480, Roche, Basel, Switzerland) to analyze the expression of pro-inflammatory mediators (*TNF-α*, *IL-1β*, and *IL-8*). Primer sequences (Sangon Bioengineering, Shanghai, China) are listed in **Supplementary Table 1**. CT values were correlated with the initial DNA copy number. Relative gene expression was calculated using the double CT value method:

$$\Delta CT = CT_{\text{target gene}} - CT_{\text{reference gene}}$$

$$\Delta\Delta CT = \Delta CT_{\text{target sample}} - \Delta CT_{\text{control}}$$

where the relative expression level of the target genes = $2^{-\Delta\Delta CT}$, and the relative expression of the control group was $2^0 = 1$.

Western blot

Briefly, the protein concentration of an aliquot of the prostate tissue homogenate was measured following the instructions of the bicinchoninic acid (BCA) kit (Sigma). Tissue samples and protein markers were subjected to sodium dodecyl sulfate-polyacrylamide gel electrophoresis (SDS-PAGE), and the separated polypeptides were transferred to polyvinylidene fluoride membranes. The membranes were soaked in Tris-buffered saline (TBS), incubated in blocking buffer (5% skim milk powder in TBS with 0.1% Tween [TBST] solution), washed with TBST solution, and incubated overnight at 4°C with monoclonal antibodies against phospho-NF-κB P65, NF-κB P65, phospho-P38, P38, and I-κBα (dilution 1:1000) or GAPDH (dilution 1:10 000). On the next day, the membranes were washed with TBST three times and incubated with goat anti-rabbit or anti-mouse IgG antibodies at room temperature for 1 h. Membranes were washed three times with TBST, then electrochemiluminescence reagent was added to visualize protein expression. Blot images were acquired on a Tanon 6600 luminous imaging workstation, and optical density was determined using Image Pro Plus 6.0 software (Media Cybernetics, Rockville, MD, USA).

Statistical analyses

Statistical analyses were performed using SPSS software 25.0 (SPSS, Chicago, IL, USA). Data are expressed as the mean ± standard deviation (s.d.), using ($x \pm s$), and n represents the number of animals. A Student's *t*-test was used for normally distributed data. One-way analysis of variance and Tukey's test were used to evaluate the statistical significance of the differences between groups. $P < 0.05$ or $P < 0.01$ was considered to indicate statistically significant results.

RESULTS

Tt-SOD reduces the PI of CP/CPPS

The PI of rats in the model group was significantly higher ($P < 0.01$) than that in the sham group, and the PI of the Tt-SOD (300 U g⁻¹ and 500 U g⁻¹) groups was significantly lower than that of the model group ($P < 0.05$ and $P < 0.01$, respectively; **Figure 1a**).

Tt-SOD improves the pain threshold of CP/CPPS

Figure 1b shows the change in the pain threshold of rats in each group during the 28-day experiments. The pain threshold of rats in each group gradually improved to some extent. Importantly, before the experiments, we measured the pain thresholds of rats in each group, and no significant initial differences were found (**Figure 1c**). On day 7, we observed a significant decrease in the pain threshold in the model group compared with that in the sham group ($P < 0.01$), whereas no significant differences were observed between the other groups and the model group (all $P > 0.05$), as shown in **Figure 1d**. On day 14, compared with that in the sham group, the pain threshold of rats in the model group was significantly lower ($P < 0.01$), and the model group had a significantly higher threshold than the Tt-SOD high-dose group

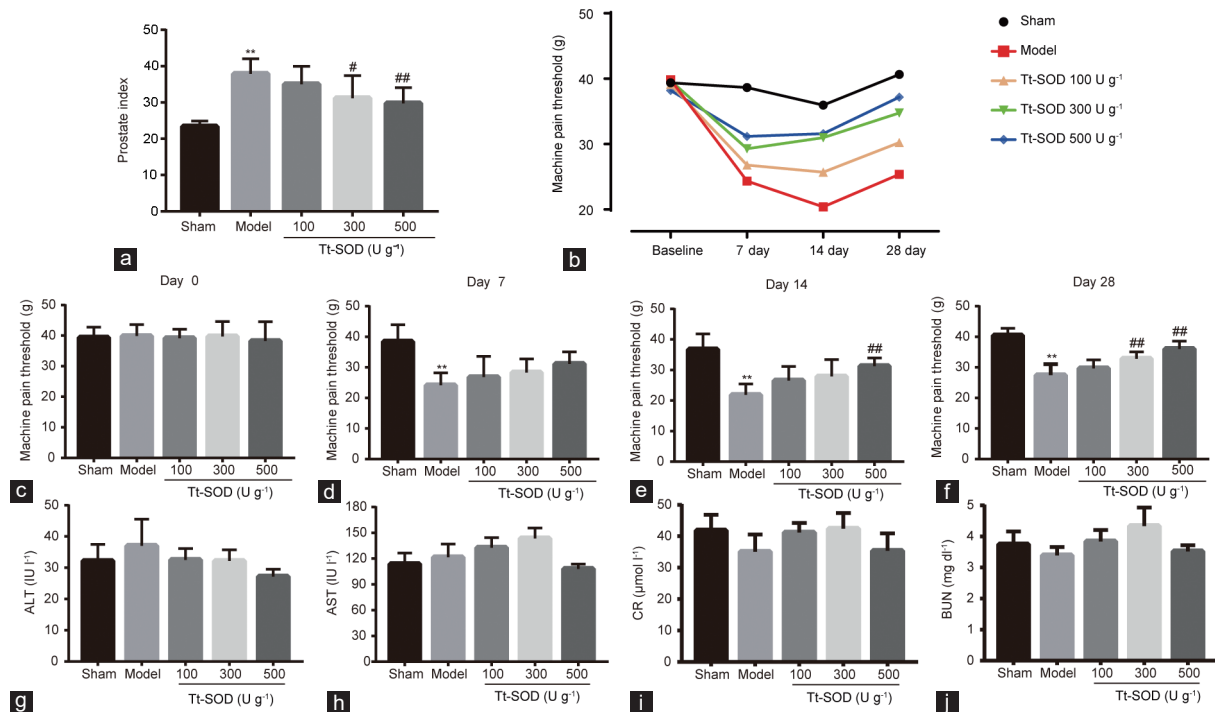


Figure 1: Comparison of prostate index and mechanical allodynia in sham group, model group, Tt-SOD 100 U g⁻¹ (low-dose) group, Tt-SOD 300 U g⁻¹ (medium-dose) group, and Tt-SOD 500 U g⁻¹ (high-dose) group. (a) Comparison of prostate index in each group; (b) change in mechanical allodynia in each group before the experiments; (c) comparison of pain thresholds in each group on day 7; (d) comparison of pain thresholds in each group on day 14; (e) comparison of pain thresholds in each group on day 28; (f) comparison of pain thresholds in each group on day 28; serum (g) ALT, (h) AST, (i) CR, and (j) BUN levels. Results are expressed as mean ± standard deviation ($n = 8$). ** $P < 0.01$, the indicated group versus sham group; # $P < 0.05$ and ## $P < 0.01$, the indicated group versus model group. ALT: alanine transaminase; AST: aspartate transaminase; CR: creatinine; BUN: blood urea nitrogen; Tt-SOD: Thermus thermophilic-superoxide dismutase.

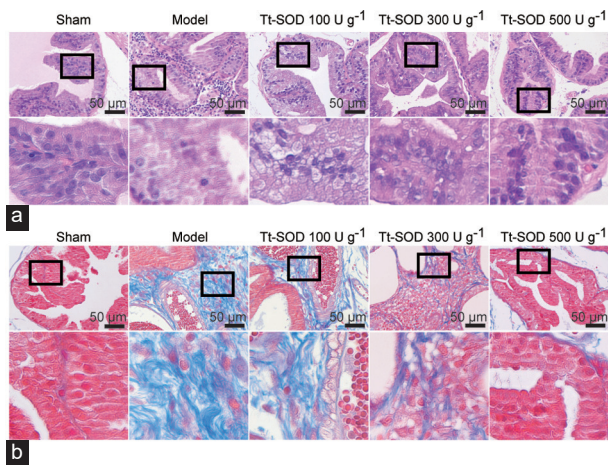


Figure 2: Representative H&E and Masson staining images from sham group, model group, Tt-SOD 100 U g⁻¹ (low-dose) group, Tt-SOD 300 U g⁻¹ (medium-dose) group, and Tt-SOD 500 U g⁻¹ (high-dose) group. (a) 400× magnification image of H&E staining for each group (upper), and extended field image (lower) in the black box of the upper image; (b) 400× magnification image of Masson staining from each group. Lower image is an extended field image in the black box of the upper image. H&E: hematoxylin and eosin; Tt-SOD: Thermus thermophilic-superoxide dismutase.

(500 U g⁻¹; $P < 0.01$; **Figure 1e**). On day 28, compared with that in the sham group, the pain threshold of rats in the model group remained significantly lower ($P < 0.01$), and those in the Tt-SOD (300 U g⁻¹ and 500 U g⁻¹) groups significantly higher than the threshold values (both $P < 0.01$), as shown in **Figure 1f**.

Tt-SOD has no significant effect on ALT, AST, CR, or BUN levels

The CR, BUN, ALT, and AST serum biochemical parameters in each group were quantified. We found no statistically significant changes in any of the assessed parameters (all $P > 0.05$; **Figure 1g–1j**).

Tt-SOD lessens tissue damage, inflammatory cell infiltration, and fibrosis

H&E staining was performed to visualize changes in prostate histological structure in each group and evaluate the therapeutic effects of Tt-SOD on CP/CPPS. In the sham group, no edema was observed in the prostate interstitium, the glandular lumen structure was intact, and the acinar epithelium was not significantly proliferative (**Figure 2a**). No inflammatory cell infiltration was observed in any of the structures. In the model group, edema, increased secretion, and vascular congestion were observed, and the prostate gland presented obvious structural abnormalities such as cavities with abnormal secretions and uneven tissue hyperplasia. Notably, the Tt-SOD (100 U g⁻¹, 300 U g⁻¹, and 500 U g⁻¹) groups showed different degrees of gland inflammation, and cavity discharge was reduced in a dose-dependent manner.

Masson staining was performed to visualize the degree of fibrosis in the prostate tissue of each group and evaluate the therapeutic effects of Tt-SOD on fibrous connective tissue during CP/CPPS. No obvious fibrosis was observed in the sham group, whereas the model group showed obvious fibrosis (**Figure 2b**). The Tt-SOD (100 U g⁻¹, 300 U g⁻¹, and 500 U g⁻¹) groups, however, exhibited different degrees of fibrosis with a dispersed distribution; with increasing Tt-SOD concentrations, the degree of fibrosis was significantly reduced in a dose-dependent manner.

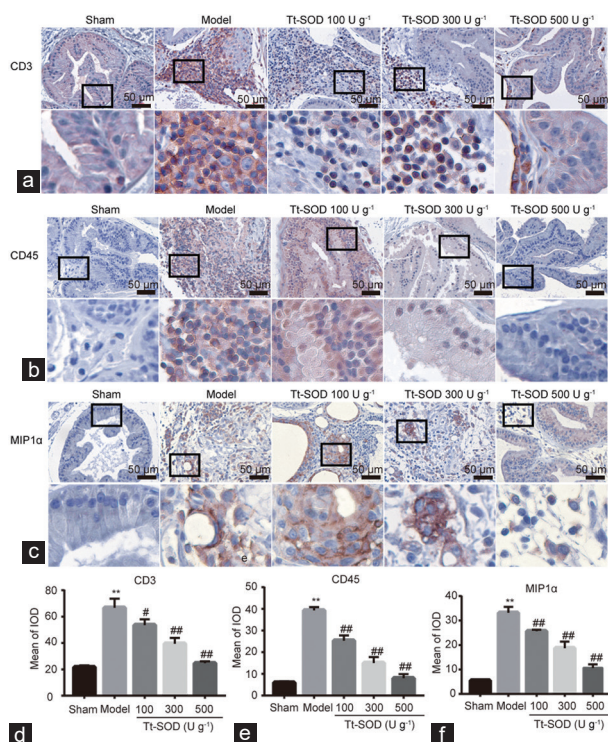


Figure 3: Immunohistochemistry of CD3, CD45, and MIP1 α cells in sham group, model group, Tt-SOD 100 U g⁻¹ (low-dose) group, Tt-SOD 300 U g⁻¹ (medium-dose) group, and Tt-SOD 500 U g⁻¹ (high-dose) group. (a) 400 \times magnification image of the immunohistochemical images of CD3 cells in each group (upper), and extended field image (lower) in the black box of the upper image; (b) 400 \times magnification of CD45 cells in each group (upper), and extended field image (lower) in the black box of the upper image; (c) 400 \times magnification of MIP1 α cells (upper), and extended field image (lower) in the black box of the upper image; quantitative comparison of (d) CD3 cells, (e) CD45 cells, and (f) MIP1 α cells in each group. ** $P < 0.01$, the indicated group versus sham group; # $P < 0.05$ and ## $P < 0.01$, the indicated group versus model group. CD3: cluster of differentiation 3; CD45: cluster of differentiation 45; MIP1 α : macrophage inflammatory protein 1 α ; IOD: integrated option density; Tt-SOD: *Thermus thermophilic*-superoxide dismutase.

Tt-SOD reduces the number of infiltrating CD3, CD45, and MIP1 α cells

To preliminarily distinguish between the inflammatory cell types that infiltrate prostate tissue during CP/PPS, IHC staining of CD3, CD45, and MIP1 α cells was performed (Figure 3a–3c). CD3 is a biomarker for T lymphocytes, CD45 is a non-specific marker for leukocytes, and MIP1 α is a biomarker for macrophages. Compared with those in the sham group, the levels of CD3, CD45, and MIP1 α in the model group were significantly increased ($P < 0.01$; Figure 3d–3f). Interestingly, compared with that in the model group, the levels of CD3, CD45, and MIP1 α in the Tt-SOD (100 U g⁻¹, 300 U g⁻¹, and 500 U g⁻¹) groups were significantly decreased (all $P < 0.05$), and there was a dose-dependent increase with Tt-SOD concentration.

Tt-SOD reduces ROS levels in prostate tissue

Oxidative stress results from an imbalance between ROS formation and endogenous antioxidant capacity, which is caused by excessive ROS production or reduced ROS scavenging. Therefore, we used the DCFH-DA probe to quantitatively analyze ROS in prostate tissues using our model of CP/PPS. As shown in Figure 4a and 4b, ROS levels in the model group were significantly higher (both $P < 0.01$) than those in the sham group; however, compared with those in the model group, ROS levels in the Tt-SOD (100 U g⁻¹, 300 U g⁻¹, and 500 U g⁻¹) groups were decreased significantly (all $P < 0.01$). These results suggest that Tt-SOD reduces oxidative damage in a dose-dependent manner.

Tt-SOD improves the antioxidant capacity of prostate tissue

To assess the antioxidant capacity in prostate tissue, we assessed the antioxidant markers MDA, NO, SOD, CAT, and GSH-PX. Compared with those in the sham group, SOD, GSH-PX, and CAT levels in the model group were significantly decreased, whereas MDA and NO levels were significantly increased ($P < 0.01$; Figure 4c–4g). However, compared with those in the model group, the levels of SOD, GSH-PX, and CAT in the Tt-SOD (100 U g⁻¹, 300 U g⁻¹, and 500 U g⁻¹) groups were significantly increased, and the levels of MDA and NO were significantly decreased (all $P < 0.05$) in a dose-dependent manner.

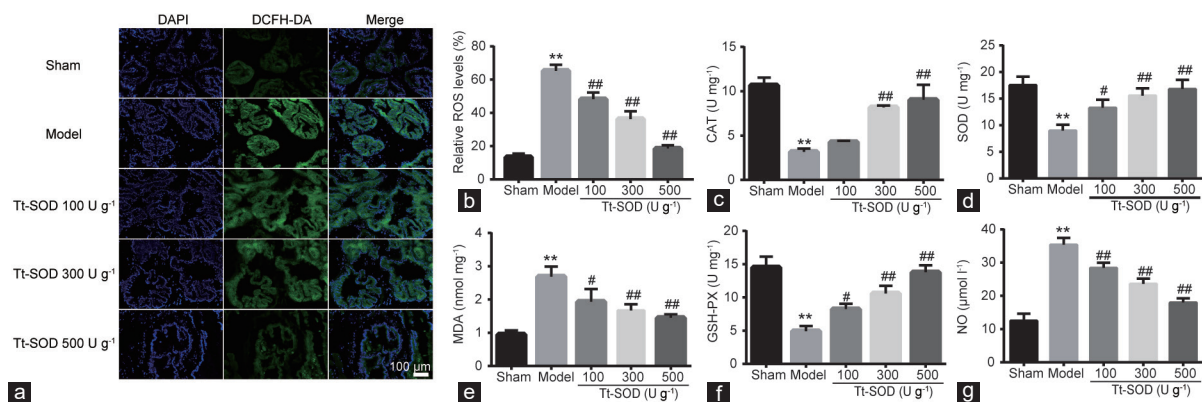


Figure 4: Comparison of indices of oxidative stress injury in sham group, model group, Tt-SOD 100 U g⁻¹ (low-dose) group, Tt-SOD 300 U g⁻¹ (medium-dose) group, and Tt-SOD 500 U g⁻¹ (high-dose) group. (a) Representative images of DCFH-DA fluorescence staining to assess ROS levels in each group; (b) quantitative analysis (green: DCFH-DA, blue: DAPI, 630 \times magnification). The levels of (c) CAT, (d) SOD, (e) MDA, (f) GSH-PX, and (g) NO in each group were detected using ELISA. Results are expressed as mean \pm standard deviation. ** $P < 0.01$, the indicated group versus sham group; # $P < 0.05$ and ## $P < 0.01$, the indicated group versus model group. CAT: catalase; DAPI: 4',6-diamidino-2-phenylindole; DCFH-DA: 2',7'-dichlorofluorescein diacetate; ELISA: enzyme-linked immunosorbent assays; GSH-PX: glutathione peroxidase; MDA: malondialdehyde; NO: nitric oxide; SOD: superoxide dismutase; Tt-SOD: *Thermophilic*-superoxide dismutase.

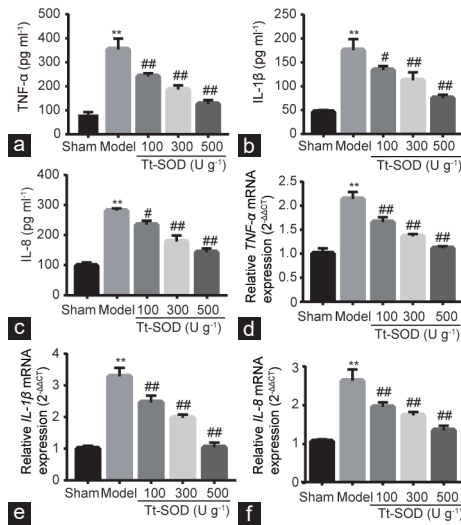


Figure 5: Expression levels of inflammatory cytokines in sham group, model group, Tt-SOD 100 U g⁻¹ (low-dose) group, Tt-SOD 300 U g⁻¹ (medium-dose) group, and Tt-SOD 500 U g⁻¹ (high-dose) group. The levels of (a) TNF-α, (b) IL-1β, and (c) IL-8 in serum samples from each group were determined using ELISA. The mRNA levels of (d) TNF-α, (e) IL-1β, and (f) IL-8 were analyzed using RT-PCR. Results are expressed as mean ± standard deviation. ***P* < 0.01, the indicated group versus sham group; #*P* < 0.05 and ##*P* < 0.01, the indicated group versus model group. TNF-α: tumor necrosis factor-α; IL-1β: interleukin-1β; IL-8: interleukin-8; ELISA: enzyme-linked immunosorbent assays; mRNA: messenger ribonucleic acid; RT-PCR: reverse transcription polymerase chain reaction; Tt-SOD: Thermus thermophilic-superoxide dismutase.

These results suggest that Tt-SOD enhances free radical scavenging and reduces peroxidation.

Tt-SOD reduces TNF-α, IL-1β, and IL-8 serum levels

To investigate the therapeutic effects of Tt-SOD on CP/CPPS in rats, we quantitatively analyzed the levels of inflammatory cytokines (TNF-α, IL-1β, and IL-8) in the serum. The levels of TNF-α, IL-1β, and IL-8 in the model group were significantly increased compared with those in the sham group (all *P* < 0.01; **Figure 5a–5c**). Compared with those in the model group, the levels of TNF-α, IL-1β, and IL-8 in the Tt-SOD (100 U g⁻¹, 300 U g⁻¹, and 500 U g⁻¹) groups were significantly decreased (all *P* < 0.05), indicating that Tt-SOD reduces inflammation.

Tt-SOD reduces TNF-α, IL-1β, and IL-8 mRNA levels

Similarly, to determine the effect of Tt-SOD on inflammatory cytokines, we determined the mRNA levels of TNF-α, IL-1β, and IL-8 in the prostate by quantitative real-time polymerase chain reaction. As shown in **Figure 5d–5f**, the mRNA expression levels of TNF-α, IL-1β, and IL-8 in the model group were significantly increased compared with those in the sham group (all *P* < 0.01). Consistent with our other findings, compared with that in the model group, Tt-SOD (100 U g⁻¹, 300 U g⁻¹, and 500 U g⁻¹) groups showed a significantly decreased expression of these cytokines (all *P* < 0.01).

Tt-SOD inhibits protein expression of the NF-κB P65 and P38 MAPK signaling pathways

It is well-known that NF-κB and P38 MAPK play important roles in the regulation of the inflammatory response and oxidative stress. P38 MAPK regulates downstream transcription factors after activation by ROS, a hyperosmotic state, or cytokines. The transcription of inflammatory factors (TNF-α, IL-1β, and IL-8) depends on the activation of NF-κB, and the activity of NF-κB is reduced by its

inhibitor, I-κBa. Therefore, we hypothesized that Tt-SOD regulates the progression of CP/CPPS in rats by inhibiting the NF-κB and P38 MAPK signaling pathways. We examined the expression of phosphorylated NF-κB P65, NF-κB P65, phosphorylated P38, P38, and I-κBa proteins in prostate tissue. NF-κB P65 and P38 phosphorylation levels were significantly increased, and I-κBa levels significantly decreased, in the model group compared with those in the sham group (all *P* < 0.01; **Figure 6a–6d**). Compared with those in the model group, NF-κB P65 and P38 phosphorylation levels were significantly decreased, and I-κBa levels significantly increased (*P* < 0.01), in the Tt-SOD (100 U g⁻¹, 300 U g⁻¹, and 500 U g⁻¹) groups. In addition, there was no significant difference in NF-κB P65 or P38 levels among the groups (**Figure 6e and 6f**). These results suggest that Tt-SOD reduces inflammatory responses and oxidative stress injury by repressing the NF-κB P65 and P38 MAPK signaling pathways.

Proposed protective signaling of Tt-SOD in the CFA-induced CP/CPPS rat model

Our western blotting results show that the alleviation of CP/CPPS by Tt-SOD may be related to the P38 MAPK and NF-κB P65 signaling pathways. Based on this, we studied the relevant literature and explored the potential mechanisms of Tt-SOD acting on CP/CPPS. The proposed mechanism can be summarized as follows: as shown in **Figure 6g**, in the resting state, NF-κB binds to its inhibitor protein I-κBa to form a complex in the cytoplasm.²⁵ When stimulated by extracellular stimuli, such as ROS and inflammatory factors, the ubiquitin-mediated degradation pathway of I-κBa is activated, resulting in NF-κB phosphorylation and entry into the nucleus.²⁶ Meanwhile, ROS and inflammatory cytokines activate the P38 MAPK signaling pathway to phosphorylate P38, and the activated P38 enters the nucleus together with activated NF-κB to regulate gene transcription and promote the release of inflammatory cytokines such as TNF-α, IL-1β, and IL-8.^{27,28} In this study, Tt-SOD catalyzed the conversion of the ROS superoxide anion radical (O^{2•-}) into hydrogen peroxide (H₂O₂), thus reducing the generation of free radicals, and H₂O₂ was converted to H₂O and O₂ under the action of ascorbic acid and catalase.²⁹ Therefore, Tt-SOD limits the effects of ROS on the P38 MAPK and NF-κB P65 signaling pathways, thereby reducing the release of inflammatory factors and suggesting that the anti-inflammatory and antioxidative stress injury effects of Tt-SOD are related to NF-κB P65 and P38 MAPK signaling.

DISCUSSION

The main findings of this study are as follows: (1) inflammatory responses and oxidative stress play important roles in the rat model of prostatitis; (2) Tt-SOD regulates the inflammatory response and oxidative stress in a CP/CPPS rat model; and (3) the NF-κB P65 and P38 MAPK signaling pathways play key roles in the ability of Tt-SOD to regulate inflammatory responses and oxidative stress injury in a rat model of CP/CPPS. These results suggest that Tt-SOD is useful for treating CP/CPPS.

Intraprostatic injection of CFA in male Sprague–Dawley rats is the most commonly reported model for inducing CP/CPPS, which was successfully employed in this study. Our results show that different concentrations of Tt-SOD improved the PI and CP/CPPS pain threshold, reduced tissue damage and tissue fibrosis, reduced free radical oxidative stress damage, and reduced inflammatory cell infiltration. Specifically, Tt-SOD reduced ROS, MDA, and NO levels, increased SOD, GSH-PX, and CAT levels, reduced the number of CD3, CD45, and MIP1α cells, and reduced serum levels of TNF-α, IL-1β, and IL-8. Based on these results, we conclude that Tt-SOD

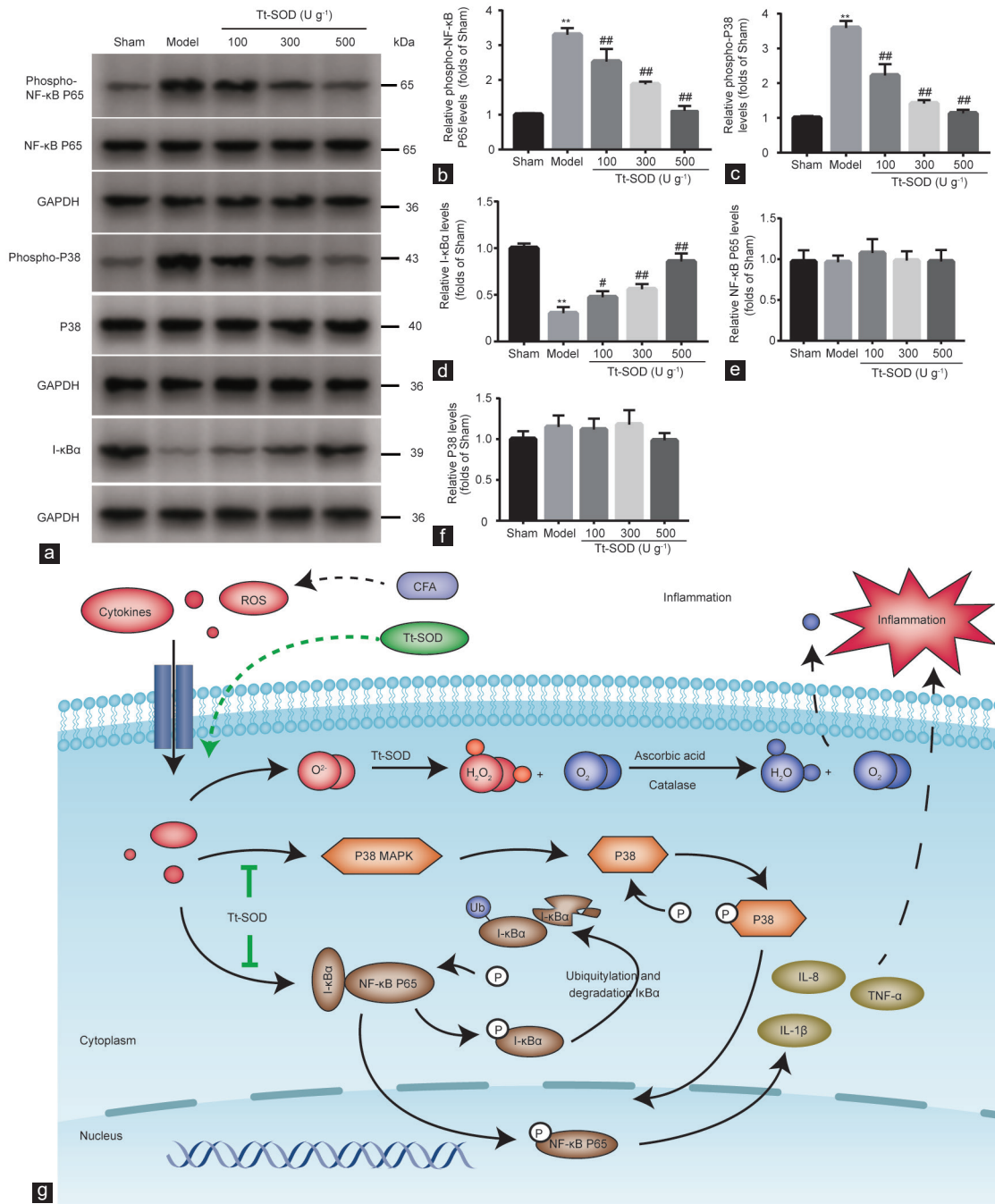


Figure 6: Western blotting analysis of sham group, model group, Tt-SOD 100 U g⁻¹ (low-dose) group, Tt-SOD 300 U g⁻¹ (medium-dose) group, and Tt-SOD 500 U g⁻¹ (high-dose) group, and schematic diagram. (a) Representative immunoblots for each group. Quantification of (b) phospho-NF-κB P65, (c) phospho-P38, (d) I-κBα, (e) NF-κB P65, and (f) P38 levels in each group. (g) Schematic diagram showing protective signaling of Tt-SOD in a CFA-induced CP/CPPS rat model. ***P* < 0.01, the indicated group versus sham group; #*P* < 0.05 and ##*P* < 0.01, the indicated group versus model group. Tt-SOD: *Thermus thermophilus*-superoxide dismutase; CFA: complete Freund's adjuvant; CP/CPPS: chronic prostatitis/chronic pelvic pain syndrome; TNF-α: tumor necrosis factor-α; IL-1β: interleukin-1β; IL-8: interleukin-8; GAPDH: glyceraldehyde-3-phosphate dehydrogenase; ROS: reactive oxygen species; MAPK: mitogen-activated protein kinase; I-κBα: inhibitor of nuclear factor-κB; NF-κB: nuclear factor-κB.

exerts anti-inflammatory and antioxidative stress effects to alleviate CP/CPPS in rats induced by CFA injection.

The pathogenesis of CP/CPPS is not completely understood. It may be related to urine reflux, nervous system disorders, abnormal immune responses, oxidative stress injury, and imbalance in sex hormone levels.^{6,30,31} In recent years, many studies have confirmed that oxidative stress injury and inflammatory cytokines are involved in the pathogenesis

of CP/CPPS.³² Under normal physiological conditions, the production and clearance of ROS in the body occurs in a dynamic equilibrium.³³ ROS metabolism disorders affect prostate inflammatory lesions, in which large amounts of ROS are produced and antioxidant enzyme activity is inhibited. These in turn cause peroxidative damage to cellular proteins, DNA, cell membranes, and organelles, leading to prostate tissue hypoxia, degeneration, edema, blood stasis, and fibrotic pathological

changes, which are associated with the occurrence and development of CP/CPPS.^{34,35} It is well-known that the overall inflammatory response depends on the balance between anti-inflammatory and pro-inflammatory mediators.³⁶ The pro-inflammatory cytokines IL-1 β and TNF- α increase prostatic secretions and semen from patients with CP/CPPS, and a large number of inflammatory cells such as granulocytes, T lymphocytes, and macrophages are observed in prostate tissue.^{37,38} Therefore, a complex cellular immune response may occur during the pathological progression of CP/CPPS.

Recent studies indicated that antioxidative and anti-inflammatory drugs or methods have protective effects against CP/CPPS to some extent. Zhao *et al.*⁷ found that quercetin alleviates prostate tissue injury in rats with CP/CPPS, reduces the expression of inflammatory cytokines (including IL-1 β , IL-2, IL-6, IL-17A, monocyte chemoattractant protein 1 [MCP1], and TNF- α), and up-regulates antioxidative markers (including total SOD [T-SOD], CAT, GSH-PX, and MDA). Using the same methods as the present study, Yang *et al.*³⁹ tested the application of XLQ[®] drugs with antioxidant abilities and observed that they reduce prostate tissue damage, the number of CD3⁺ T cells, CD45⁺ leukocyte infiltration, and inflammatory cytokine levels (including IL-1 β , IL-2, IL-6, IL-17A, TNF- α , and MCP1), as well as improve the antioxidative capacity through increased total superoxide dismutase (T-SOD CAT, and GSH-PX levels and decreased MDA levels). Similarly, Chen *et al.*⁴⁰ and Fu *et al.*⁴¹ used different drugs or methods to target inflammation and oxidative stress in prostate tissue, and showed a mitigating role of inflammation and oxidative stress in a rat model of CP/CPPS. Pro-inflammatory cytokines and oxidative stress are the main factors leading to the phosphorylation of NF- κ B and P38 MAPK, which then promote the production of inflammatory cytokines and further aggravate the oxidative stress. In the present study, we applied Tt-SOD, the anti-inflammatory and antioxidative stress effects of which were confirmed in our previous studies.¹⁶ Our results also show that Tt-SOD diminished tissue inflammation and oxidative stress damage during CP/CPPS. The NF- κ B P65 and P38 MAPK pathways are chronically active in many inflammatory diseases such as arthritis, inflammatory bowel disease, gastritis, and sepsis.^{42,43} Our results suggest that Tt-SOD inhibits the NF- κ B P65 and P38 MAPK signaling pathways, thereby playing an anti-inflammatory and antioxidative role.

CONCLUSIONS

Tt-SOD alleviated the inflammatory response and oxidative stress injury in a rat model of autoimmune prostatitis, thus presenting an effective therapeutic option for CP/CPPS that should be further evaluated. However, a limitation of this study is that we only examined these effects in animals, and the mechanism of action of Tt-SOD on CP/CPPS in humans requires further analysis. In our future studies, we will establish a suitable cell model for exploring the effects of Tt-SOD on prostate cells.

AUTHOR CONTRIBUTIONS

NWC, JJ, and LFW were responsible for the conceptualization of the study. NWC, HX, XCW, WHX, and YXC performed the experiment. NWC, JJ, and JLG performed the data analyses and wrote the original draft of the paper. YH and JLG helped to improve the paper with constructive discussions. All authors read and approved the final manuscript.

COMPETING INTERESTS

All authors declare no competing interests.

ACKNOWLEDGMENTS

We thank Dr. Fan-Guo Meng and Hangzhou Redox Pharmatech Co., Ltd. (Hangzhou, China) for providing the purified Tt-SOD. We would like to thank our colleagues in the Pathology Department of the Affiliated Hospital of Jiaxing University for their intellectual inspiration and technical assistance. The present study was supported by the Medical Scientific Research Foundation of Zhejiang Province (2021RC129, and 2019KY694), the National Natural Science Foundation of China (82000230), the Jiaxing Medical Key Subject Funding of Zhejiang Province (2019-zc-07), and the Jiaxing Key Laboratory of Precise Diagnosis and Treatment of Urological Tumor (2020-mnzdsys).

Supplementary Information is linked to the online version of the paper on the *Asian Journal of Andrology* website.

REFERENCES

- Fan S, Hao Z, Zhang L, Zhou J, Zhang YF, *et al.* ASIC1a contributes to the symptom of pain in a rat model of chronic prostatitis. *Asian J Androl* 2018; 20: 300–5.
- Huang T, Wang G, Hu Y, Shi H, Wang K, *et al.* Structural and functional abnormalities of penile cavernous endothelial cells result in erectile dysfunction at experimental autoimmune prostatitis rat. *J Inflamm* 2019; 16: 20.
- Liu X, Ran X, Riaz M, Kuang H, Dou D, *et al.* Mechanism investigation of *Tagetes patula* L. against chronic nonbacterial prostatitis by metabolomics and network pharmacology. *Molecules* 2019; 24: 2266.
- Wang J, Yang J, Deng S, Yu XD, Bao BH, *et al.* Acupuncture combined with tamsulosin hydrochloride sustained-release capsule in the treatment of chronic prostatitis/chronic pelvic pain syndrome: a study protocol for a randomized controlled trial. *Medicine* 2020; 99: e19540.
- Du H, Chen X, Zhang L, Liu Y, Zhan CS, *et al.* Microglial activation and neurobiological alterations in experimental autoimmune prostatitis-induced depressive-like behavior in mice. *Neuropsychiatr Dis Treat* 2019; 15: 2231–45.
- Tang M, Ullah R, Wazir J, Khan FU, Ihsan AU, *et al.* Effect of oral T2 antigen on chronic prostatitis/chronic pelvic pain syndrome in mice model. *Inflammation* 2019; 42: 2086–94.
- Zhao Q, Yang F, Meng L, Chen D, Wang M, *et al.* Lycopene attenuates chronic prostatitis/chronic pelvic pain syndrome by inhibiting oxidative stress and inflammation via the interaction of NF- κ B, MAPKs, and Nrf2 signaling pathways in rats. *Andrology* 2020; 8: 747–55.
- Abedon ST. Use of phage therapy to treat long-standing, persistent, or chronic bacterial infections. *Adv Drug Deliv Rev* 2019; 145: 18–39.
- Paulis G. Inflammatory mechanisms and oxidative stress in prostatitis: the possible role of antioxidant therapy. *Res Rep Urol* 2018; 10: 75–87.
- Zhuang C, Wang Y, Zhang Y, Nanwei X. Oxidative stress in osteoarthritis and antioxidant effect of polysaccharide from *Angelica sinensis*. *Int J Biol Macromol* 2018; 115: 281–6.
- Kim M, Jung J, Jeong NY, Chung HJ. The natural plant flavonoid apigenin is a strong antioxidant that effectively delays peripheral neurodegenerative processes. *Anat Sci Int* 2019; 94: 285–94.
- Yang C, Xia W, Liu X, Lin J, Wu A. Role of TXNIP/NLRP3 in sepsis-induced myocardial dysfunction. *Int J Mol Med* 2019; 44: 417–26.
- You L, Yang C, Du Y, Liu Y, Chen G, *et al.* Matrine exerts hepatotoxic effects via the ROS-dependent mitochondrial apoptosis pathway and inhibition of Nrf2-mediated antioxidant response. *Oxid Med Cell Longev* 2019; 2019: 1045345.
- Kwon M, Lee K, Ham W, Tak LJ, Agrahari G, *et al.* Pathologic properties of SOD3 variant R213G in the cardiovascular system through the altered neutrophils function. *PLoS One* 2020; 15: e0227449.
- Xu F, Fan Y, Miao F, Hu GR, Sun J, *et al.* Naphthylacetic acid and tea polyphenol application promote biomass and lipid production of nervonic acid-producing microalgae. *Front Plant Sci* 2018; 9: 506.
- Yang S, Li H, Liu M, Xie B, Wei W, *et al.* A manganese-superoxide dismutase from *Thermus thermophilus* HB27 suppresses inflammatory responses and alleviates experimentally induced colitis. *Inflamm Bowel Dis* 2019; 25: 1644–55.
- Peng X, Guo H, Chen J, Wang J, Huang J. The effect of piperidone on rat chronic prostatitis/chronic pelvic pain syndrome and its mechanisms. *Prostate* 2020; 80: 917–25.
- Jin X, Lin T, Yang G, Cai H, Tang B, *et al.* Use of Tregs as a cell-based therapy via CD39 for benign prostate hyperplasia with inflammation. *J Cell Mol Med* 2020; 24: 5082–96.
- Cheng Y, Cao Y, Ihsan AU, Kahn FU, Li X, *et al.* Novel treatment of experimental autoimmune prostatitis by nanoparticle-conjugated autoantigen peptide T2. *Inflammation* 2019; 42: 1071–81.
- Ni H, Wang Y, An K, Liu Q, Xu L, *et al.* Crosstalk between NF κ B-dependent astrocytic CXCL1 and neuron CXCR2 plays a role in descending pain facilitation. *J Neuroinflammation* 2019; 16: 1.
- Yang S, Traore Y, Jimenez C, Ho EA. Autophagy induction and PDGFR- β knockdown



- by siRNA-encapsulated nanoparticles reduce Chlamydia trachomatis infection. *Sci Rep* 2019; 9: 1306.
- 22 Huang T, Zhou X, Mao X, Yu C, Zhang Z, *et al*. Lactate-fueled oxidative metabolism drives DNA methyltransferase 1-mediated transcriptional co-activator with PDZ binding domain protein activation. *Cancer Sci* 2020; 111: 186–99.
- 23 Qi Q, Dong Z, Sun Y, Li S, Zhao Z. Protective effect of bergenin against cyclophosphamide-induced immunosuppression by immunomodulatory effect and antioxidation in Balb/c mice. *Molecules* 2018; 23: 2668.
- 24 Zhang G, Kang Y, Zhou C, Cui R, Jia M, *et al*. Amelioratory effects of testosterone propionate on age-related renal fibrosis via suppression of TGF- β 1/Smad signaling and activation of Nrf2-ARE signaling. *Sci Rep* 2018; 8: 10726.
- 25 Yang HL, Hsieh PL, Hung CH, Cheng HC, Chou WC, *et al*. Early moderate intensity aerobic exercise intervention prevents doxorubicin-caused cardiac dysfunction through inhibition of cardiac fibrosis and inflammation. *Cancers (Basel)* 2020; 12: 1102.
- 26 Daniel J, Liebau E. The ufm1 cascade. *Cells* 2014; 3: 627–38.
- 27 Lee MK, Al Sharea A, Shihata WA, Bertuzzo Veiga C, Cooney OD, *et al*. Glycolysis is required for LPS-induced activation and adhesion of human CD14⁺CD16⁺ monocytes. *Front Immunol* 2019; 10: 2054.
- 28 Shin JW, Kwon SH, Choi JY, Na JI, Huh CH, *et al*. Molecular mechanisms of dermal aging and antiaging approaches. *Int J Mol Sci* 2019; 20: 2126.
- 29 Ferreira de Sousa PV, de Moraes Guimarães Y, Pinto GC, Fernando de Oliveira A, Alberto da Silva A, *et al*. Study of Cu NPs reactivity for compounds with different chemical structures: black reactive dye 5, picric acid and 2,4-D herbicide. *Chemosphere* 2019; 235: 749–56.
- 30 Wang H, Tyagi P, Chen Y, Chancellor MB, Chuang YC, *et al*. Low energy shock wave therapy inhibits inflammatory molecules and suppresses prostatic pain and hypersensitivity in a capsaicin induced prostatitis model in rats. *Int J Mol Sci* 2019; 20: 4777.
- 31 Penna G, Mondaini N, Amuchastegui S, Innocenti SD, Carini M, *et al*. Seminal plasma cytokines and chemokines in prostate inflammation: interleukin 8 as a predictive biomarker in chronic prostatitis/chronic pelvic pain syndrome and benign prostatic hyperplasia. *Eur Urol* 2007; 51: 524–33.
- 32 Snow DC, Shoskes DA. Pharmacotherapy of prostatitis. *Expert Opin Pharmacother* 2010; 11: 2319–30.
- 33 Gu Y, Han J, Jiang C, Zhang Y. Biomarkers, oxidative stress and autophagy in skin aging. *Ageing Res Rev* 2020; 59: 101036.
- 34 Xia W, Liu G, Shao Z, Xu E, Yuan H, *et al*. Toxicology of tramadol following chronic exposure based on metabolomics of the cerebrum in mice. *Sci Rep* 2020; 10: 11130.
- 35 Parma L, Peters HA, Baganha F, Sluimer JC, de Vries MR, *et al*. Prolonged hyperoxygenation treatment improves vein graft patency and decreases macrophage content in atherosclerotic lesions in ApoE3⁺Leiden mice. *Cells* 2020; 9: 336.
- 36 Azab A, Nassar A, Azab A. Anti-inflammatory activity of natural products. *Molecules* 2016; 21: 1321.
- 37 Luzzi GA. Chronic prostatitis and chronic pelvic pain in men: aetiology, diagnosis and management. *J Eur Acad Dermatol Venereol* 2010; 16: 253–6.
- 38 Khadra A, Fletcher P, Luzzi G, Shattock R, Hay P. Interleukin-8 levels in seminal plasma in chronic prostatitis/chronic pelvic pain syndrome and nonspecific urethritis. *BJU Int* 2006; 97: 1043–6.
- 39 Yang F, Meng L, Han P, Chen D, Wang M, *et al*. New therapy with XLQ to suppress chronic prostatitis through its anti-inflammatory and antioxidative activities. *J Cell Physiol* 2019; 234: 17570–7.
- 40 Chen H, Xie Y, Deng C, Zhang C, Lv L, *et al*. The anti-inflammatory and antioxidative effects of ningmitai capsule in the experimental autoimmune prostatitis rat model. *Evid Based Complement Alternat Med* 2020; 2020: 5847806.
- 41 Fu X, He H, Li C, Jiang SY, Ge HW, *et al*. Micro-RNA-155 deficiency attenuates inflammation and oxidative stress in experimental autoimmune prostatitis in a TLR4-dependent manner. *Kaohsiung J Med Sci* 2020; 36: 712–20.
- 42 Kim AT, Kim D. Anti-inflammatory effects of vanadium-binding protein from *Halocynthia roretzi* in LPS-stimulated RAW264.7 macrophages through NF- κ B and MAPK pathways. *Int J Biol Macromol* 2019; 133: 732–8.
- 43 Acikara OB, Hošek J, Babula P, Cvačka J, Budešínský M, *et al*. Turkish Scorzonera species extracts attenuate cytokine secretion via inhibition of NF- κ B activation, showing anti-inflammatory effect *in vitro*. *Molecules* 2015; 21: E43.

This is an open access journal, and articles are distributed under the terms of the Creative Commons Attribution-NonCommercial-ShareAlike 4.0 License, which allows others to remix, tweak, and build upon the work non-commercially, as long as appropriate credit is given and the new creations are licensed under the identical terms.

©The Author(s)(2021)



Supplementary Table 1: Primers used in quantitative real-time polymerase chain reaction

<i>Primer</i>		<i>Sequence (5'→3')</i>
<i>TNF-α</i>	Forward	5'-GGCTTTCGGAACACTCACTGGA-3'
	Reverse	5'-GGGAACAGTCTGGGAAGCTC-3'
<i>IL-1β</i>	Forward	5'-TTGAGTCTGCACAGTCCCC-3'
	Reverse	5'-TCCTGGGGAAGGCATTAGGA-3'
<i>IL-8</i>	Forward	5'-ACTGAGAGTGATTGAGAGTGGACC-3'
	Reverse	5'-ACCCTCTGCACCCAGTTTTC-3'
<i>GAPDH</i>	Forward	5'-GCATCTTCTGTGCAGTGCC-3'
	Reverse	5'-TACGGCCAAATCCGTTCA-3'

TNF- α : tumor necrosis factor- α ; IL-1 β : interleukin-1 β ; IL-8: interleukin-8;
GAPDH: glyceraldehyde-3-phosphate dehydrogenase